

Electronic Supplementary Information

Large-Scale Room-Temperature Synthesis and Optical Properties of Perovskite-Related Cs₄PbBr₆ Fluorophors

Daqin Chen*, Zhongyi Wan, Xiao Chen, Yongjun Yuan, Jiasong Zhong

College of Materials & Environmental Engineering, Hangzhou Dianzi University,
Hangzhou, 310018, P. R. China

E-Mail: dqchen@hdu.edu.cn

Table S1 Summary of products via IIR reaction by changing polarity of 'oil phase'

Oil Phase	Aqueous Phase	Crystalline Phase
n-hexane	DMF	Pure Cs ₄ PbBr ₆
n-heptane		Pure Cs ₄ PbBr ₆
p-xylene		Cs ₄ PbBr ₆ (major) + CsPbBr ₃
toluene		Cs ₄ PbBr ₆ + CsPbBr ₃
ethyl acetate		Cs ₄ PbBr ₆ + CsPbBr ₃ (major)
tert-butyl alcohol		Pure CsPbBr ₃

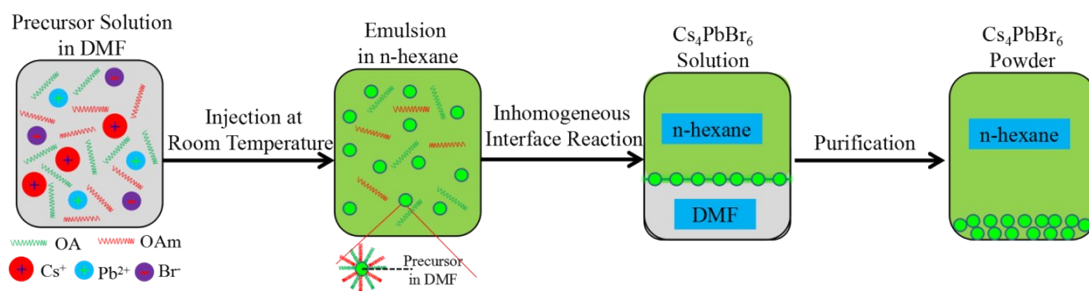


Figure S1 Schematic diagram of Cs_4PbBr_6 synthesizing process via inhomogeneous interface reaction.

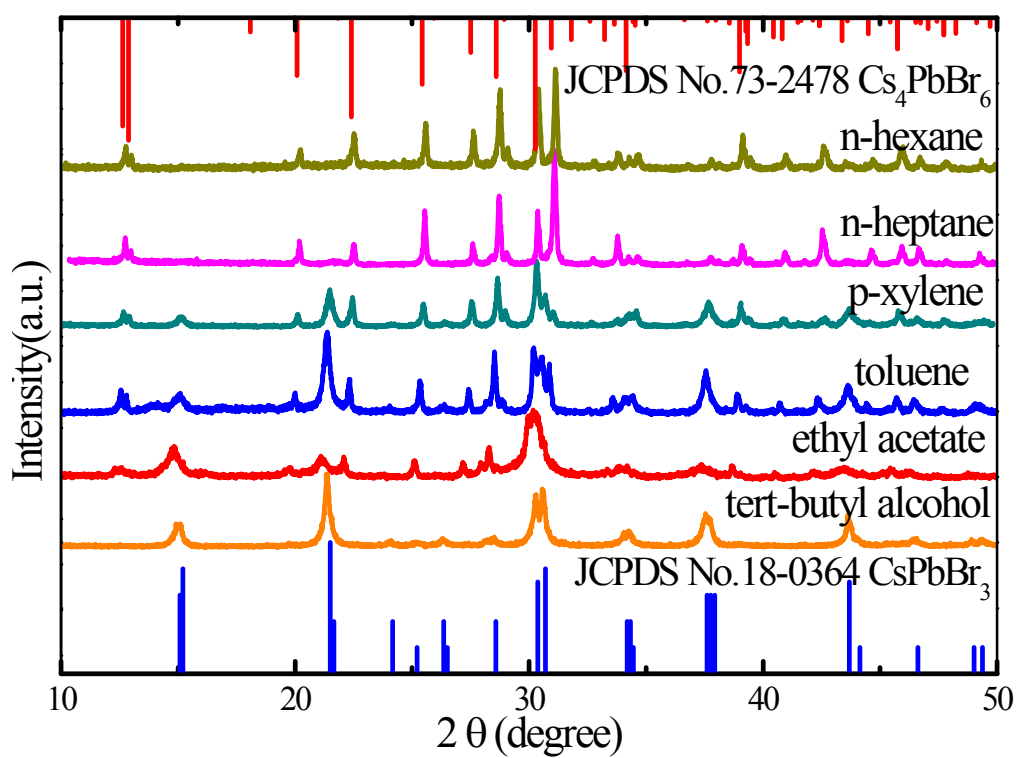


Figure S2 XRD patterns of the products using different solvents as ‘oil phase’.

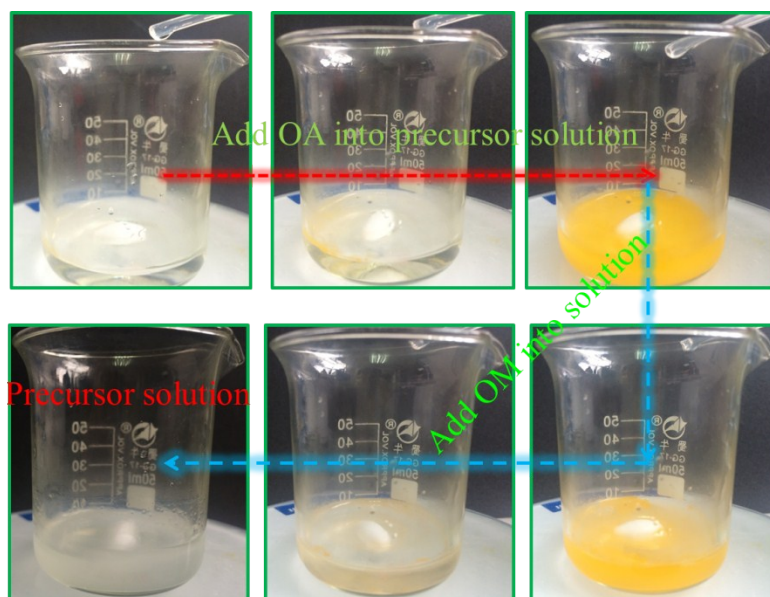


Figure S3 Photographs of the precursor solution with the addition of only OM (top) and both OM and OA (bottom), showing that OM is indispensable to protect Cs^+ , Pb^{2+} , and Br^- in precursor solution.

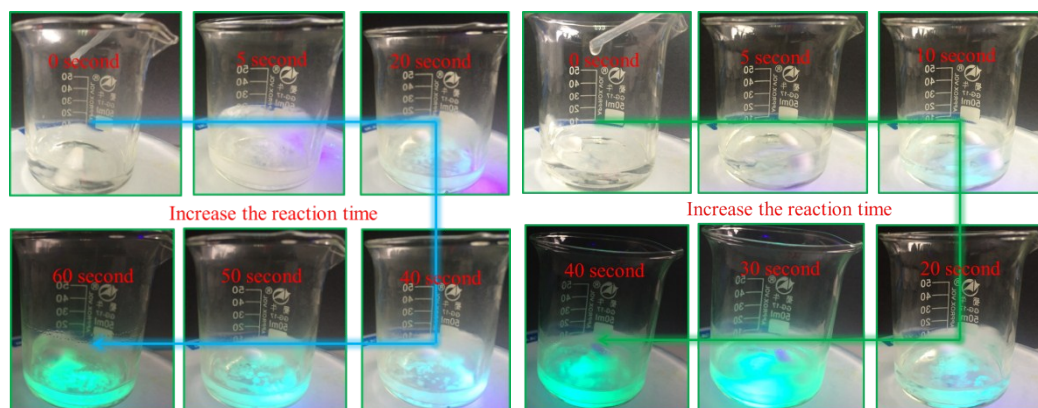


Figure S4 Luminescent photographs of the reaction system with the addition of OM (left) and both OM and OA (right) under UV illumination, showing that OA can accelerate the reaction to achieve the final products.

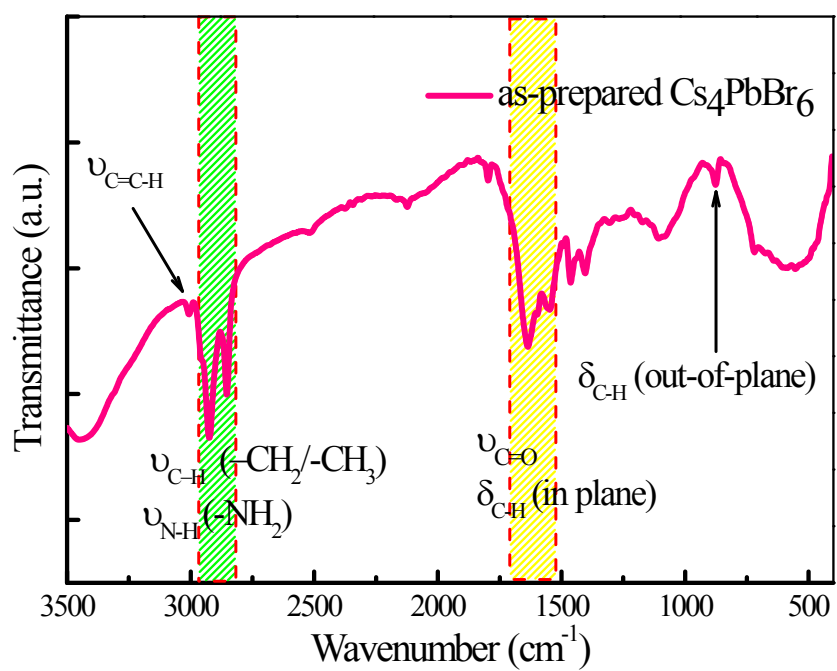


Figure S5 FTIR spectrum of the as-prepared Cs_4PbBr_6 sample.

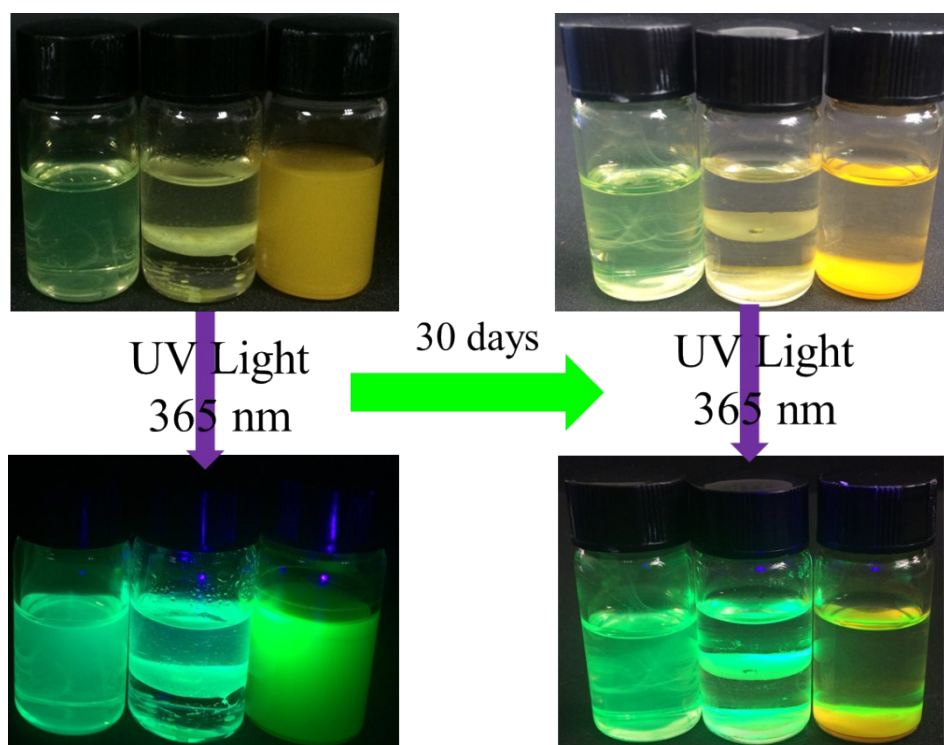
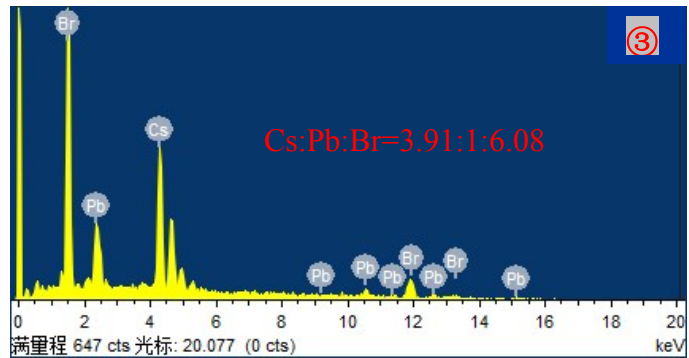
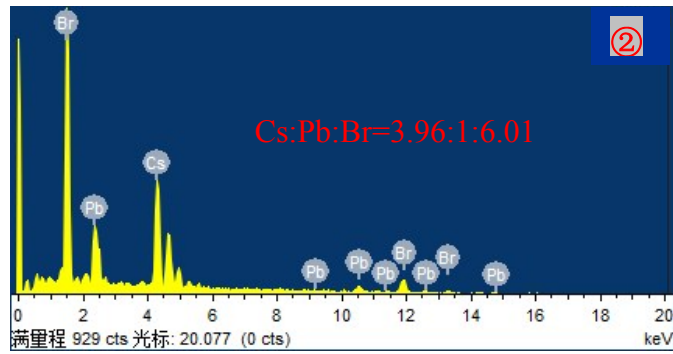
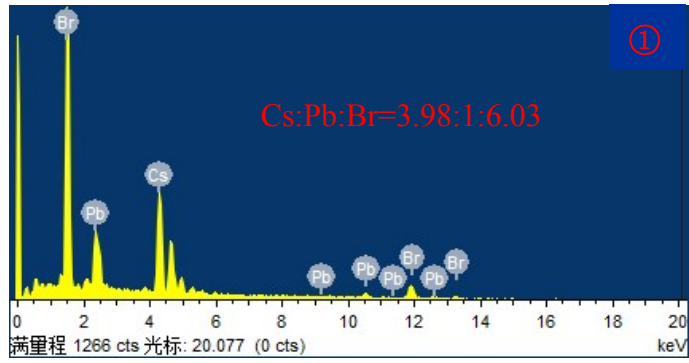
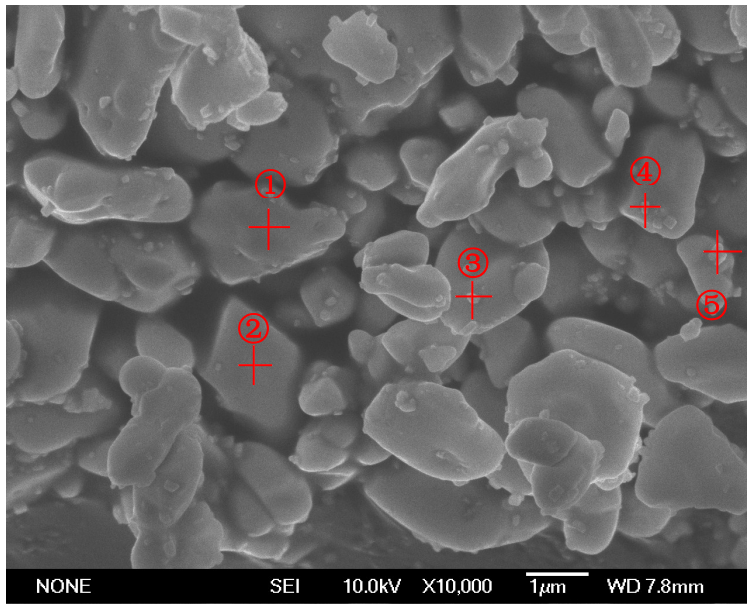


Figure S6 Photographs of the fresh products (left) and the corresponding samples stored for 30 days (right) under daylight and UV light irradiation. These three samples are prepared by using different solvents as ‘oil phase’ (from left to right: middle-polar toluene, weak-polar n-hexane and strong-polar tert-butyl alcohol).



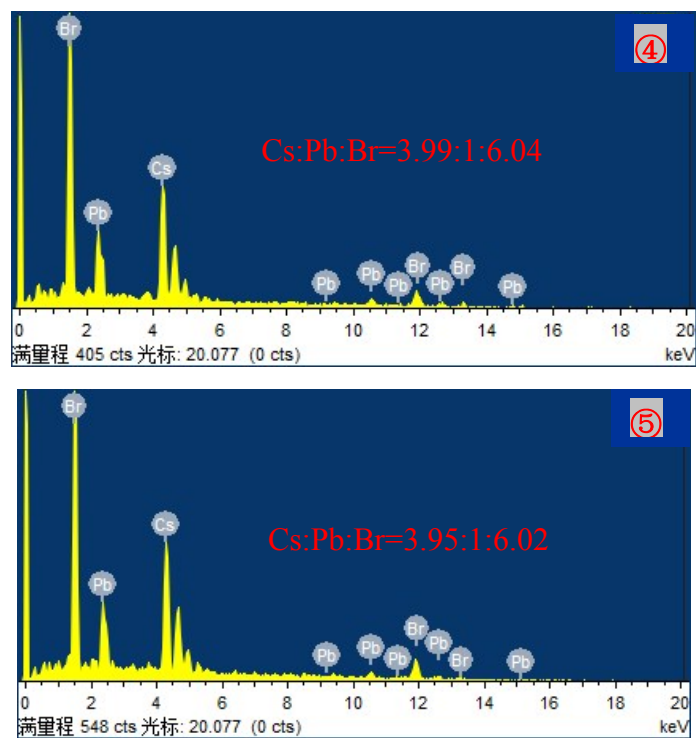


Figure S7 SEM image and EDS spectra of Cs_4PbBr_6 sample by detecting different regions, showing the approximate atomic ratio of 4:1:6 for the Cs_4PbBr_6 sample.

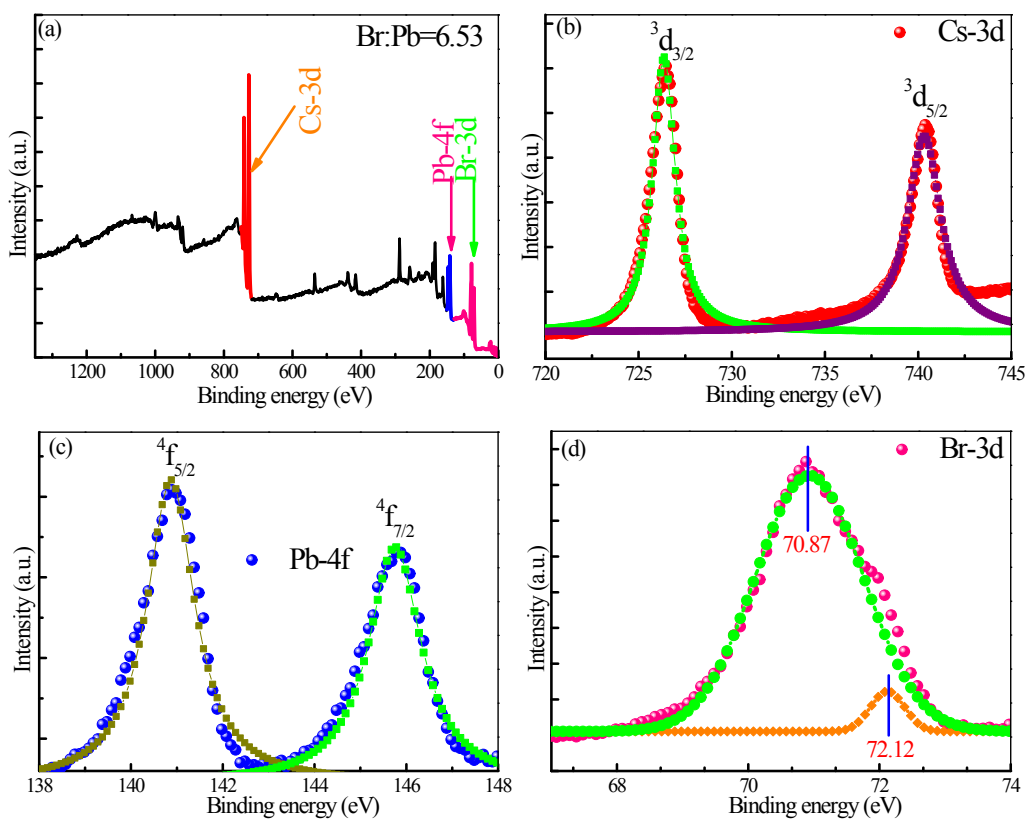


Figure S8 (a) XPS full spectrum of Cs_4PbBr_6 sample. High-resolution XPS spectra of (b) Cs-3d, (c) Pb-4f and (d) Br-3d states.

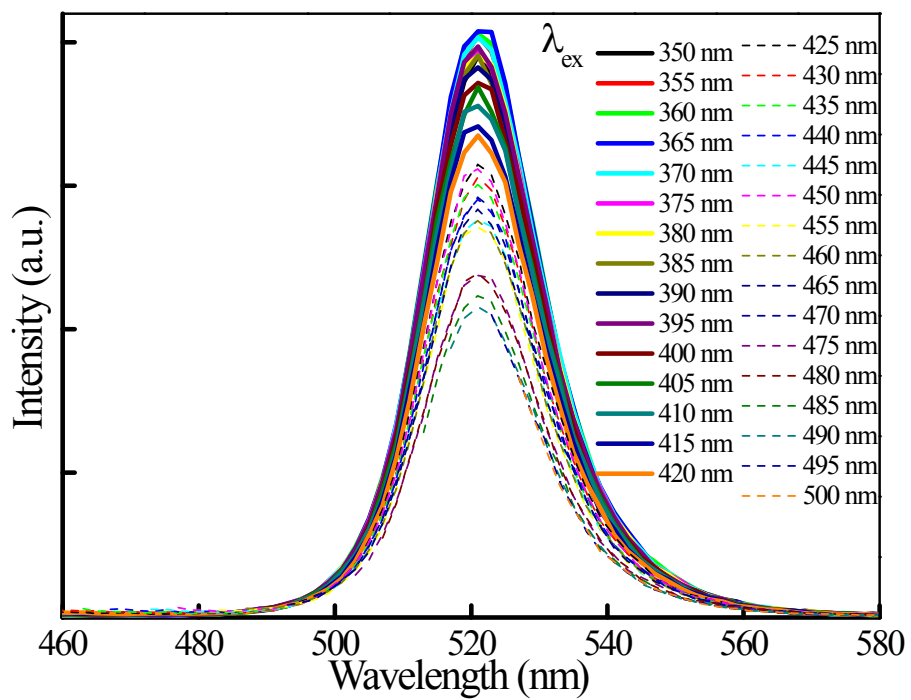


Figure S9 PL spectra recorded under the excitation of diverse wavelength lights ranging from 350 to 500 nm.

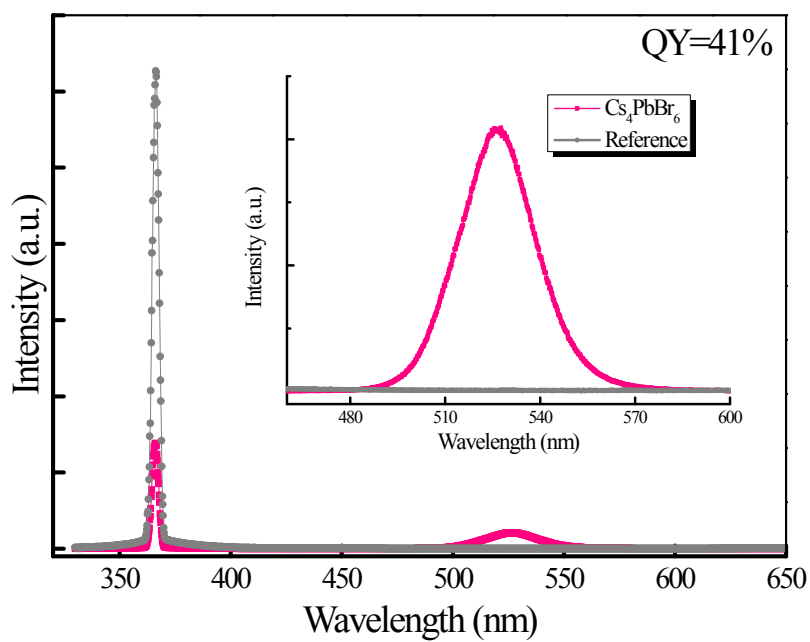


Figure S10 Quantitative excitation and emission spectra of Cs_4PbBr_6 and reference samples recorded by a spectrofluorometer equipped with an integrating sphere for QY measurement. Inset shows the magnified emission spectra in the wavelength range of 450-600 nm.

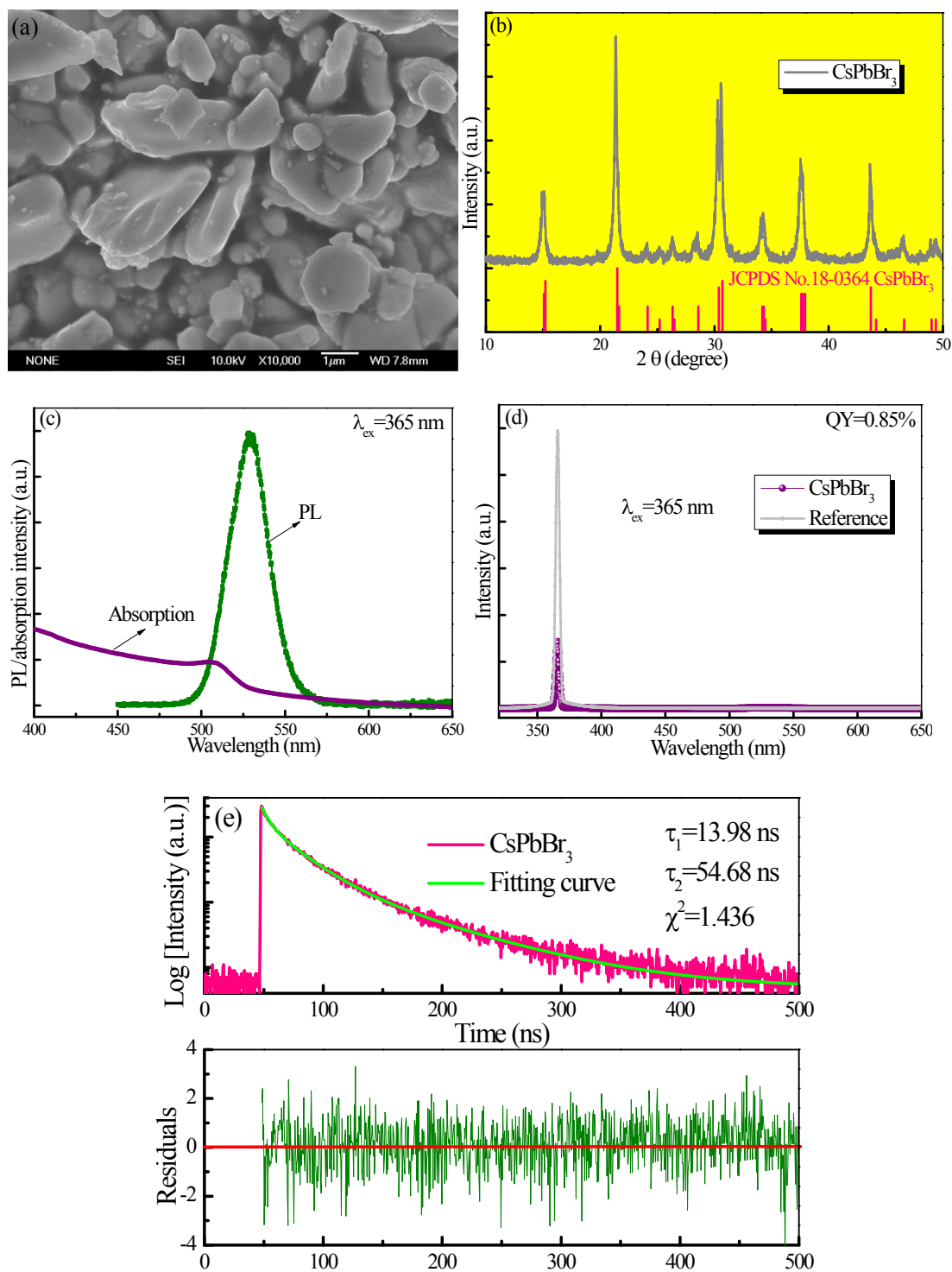


Figure S11 Structural and spectral characterizations of the fabricated CsPbBr₃ sample: (a) SEM image, (b) XRD pattern, (c) PL/absorption, (d) QY measurement and (e) decay curve.

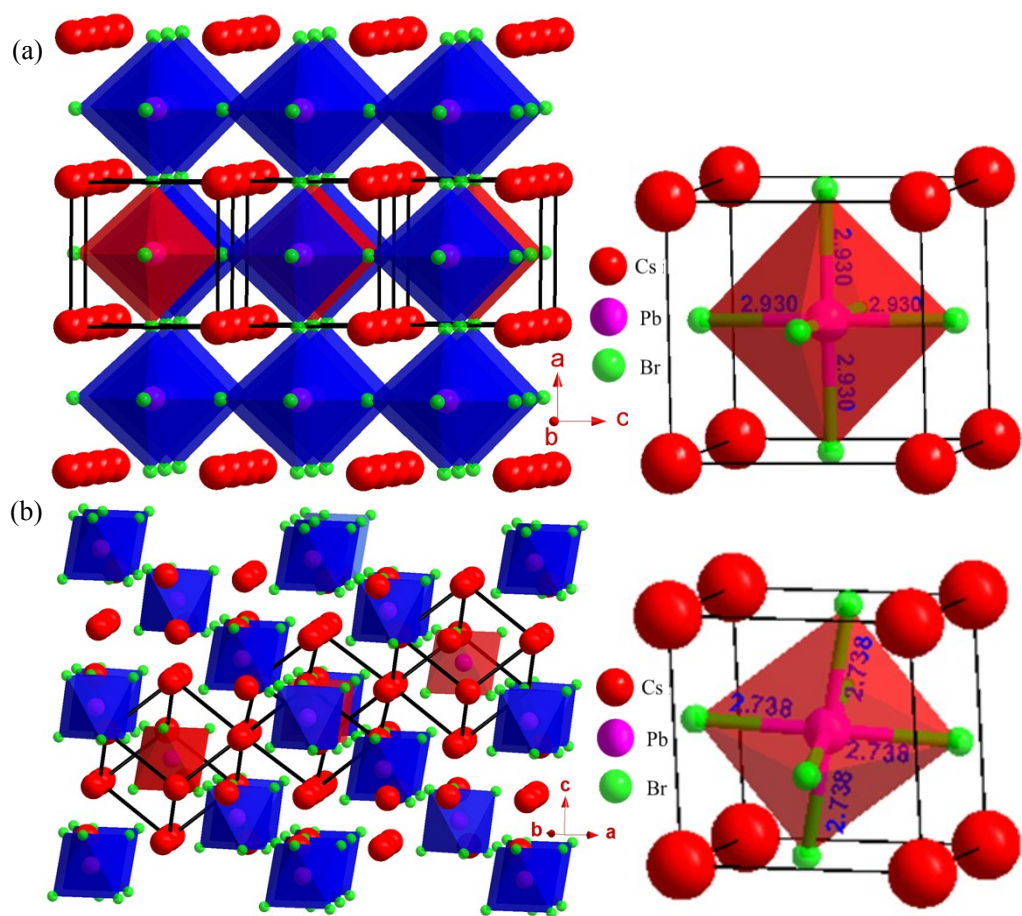


Figure S12 Schematic illustration of (a) monoclinic CsPbBr_3 and (b) rhombohedral Cs_4PbBr_6 crystal structures. PbBr_6^{4-} octahedral geometries in Cs^+ simple cubic lattices are also provided.

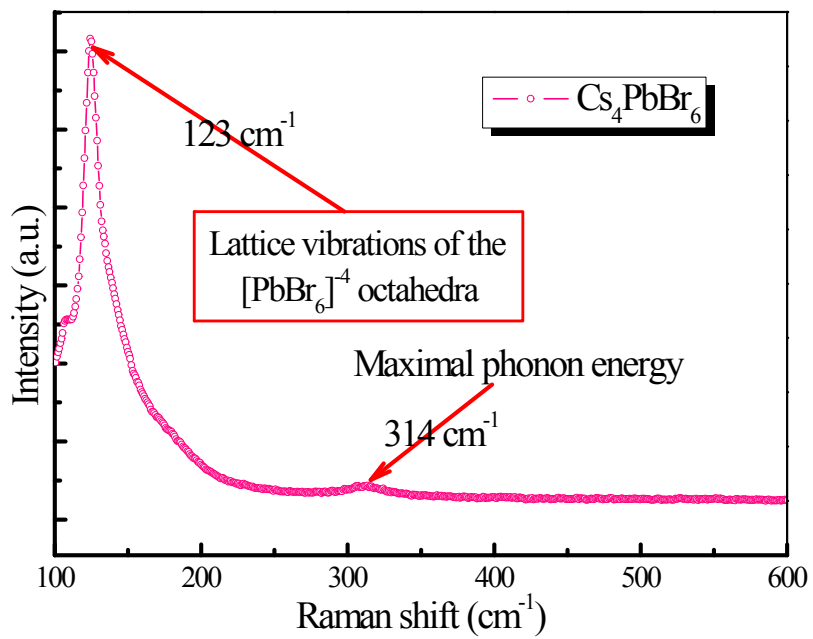


Figure S13 Raman spectrum of Cs_4PbBr_6 sample

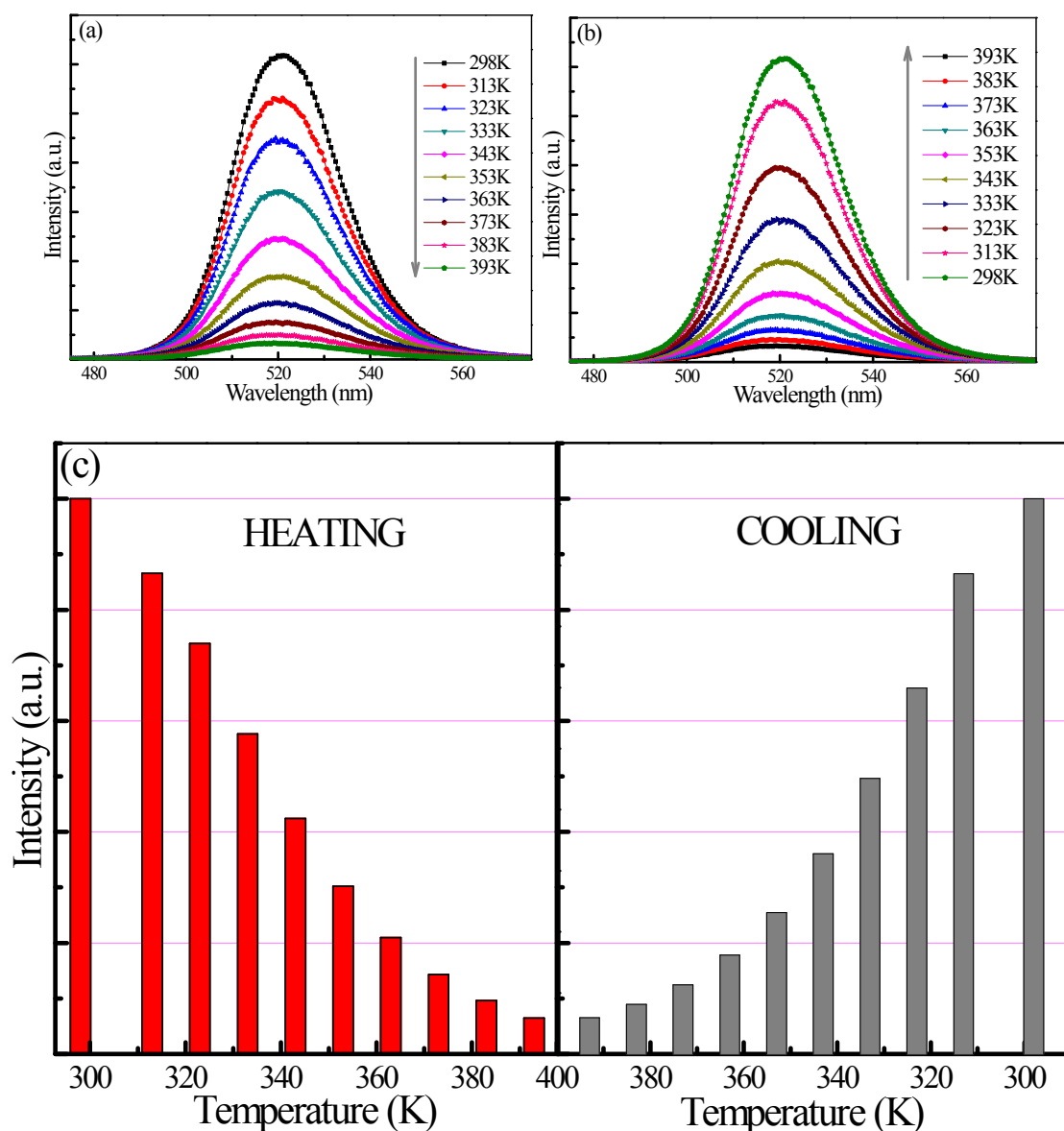


Figure S14 Temperature-dependent PL spectra on cycling processes of heating (a) and cooling (b) in the temperature range from 298 K to 393 K. (c) The corresponding PL integrated intensity as a function of temperature.

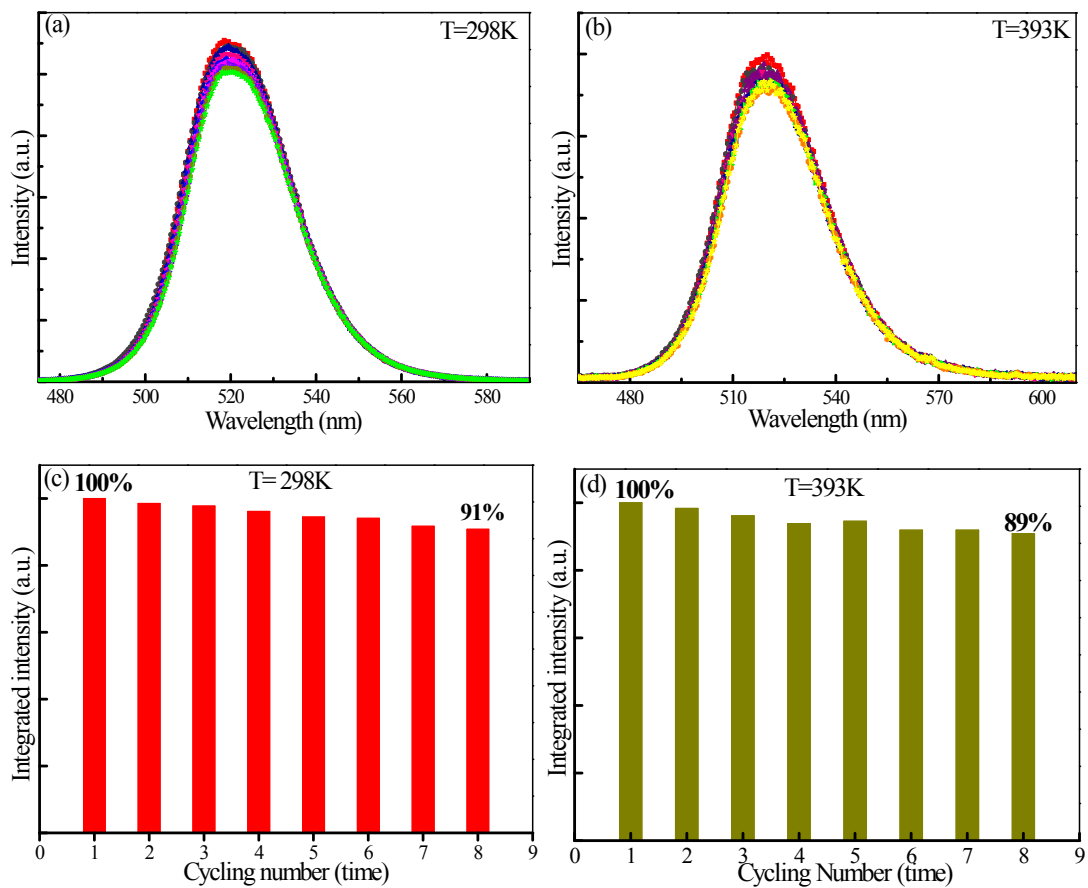


Figure S15 PL spectra and the corresponding integrated intensity of the Cs_4PbBr_6 sample recorded at the (a, c) 298 K and (b, d) 393 K respectively after eight-time cycling experiments.

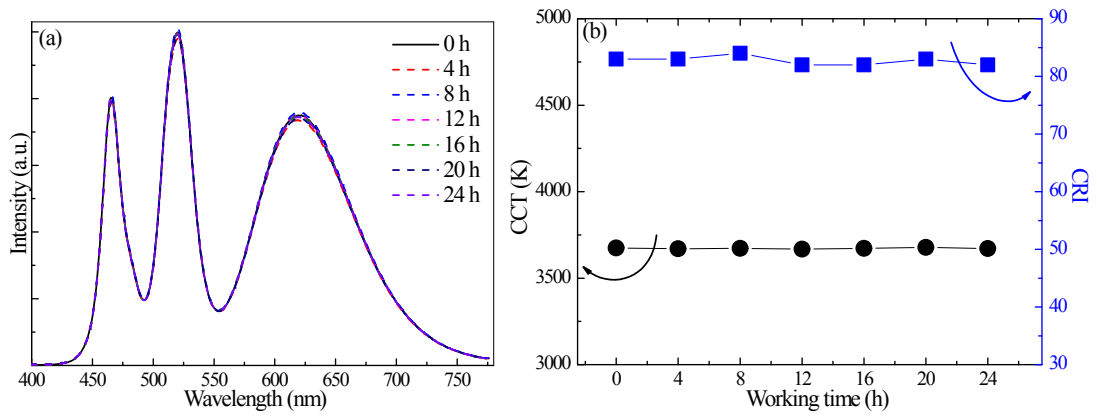


Figure S16 (a) Electroluminescence spectra of WLED at different working time intervals. (b) The related CCT and CRI versus working time intervals.